ACS APPLIED MATERIALS & INTERFACES

Research Article

www.acsami.org

Enhanced Radiation Therapy with Multilayer Microdisks Containing Radiosensitizing Gold Nanoparticles

Peipei Zhang,[†] Yong Qiao,[†] Junfei Xia,[§] Jingjiao Guan,[§] Liyuan Ma,*[,†] and Ming Su*[,†]

[†]Department of Chemical Engineering, Northeastern University, Boston, Massachusetts 02115, United States

[§]Department of Chemical and Biomedical Engineering, Florida State University, Tallahassee, Florida 32310, United States

ABSTRACT: A challenge of X-ray radiation therapy is that high dose X-rays at therapeutic conditions damage normal cells. This paper describes the use of gold nanoparticle-loaded multilayer microdisks to enhance X-ray radiation therapy, where each microdisk contains over 10^5 radiosensitizing nanoparticles. The microdisks are attached on cell membranes through electrostatic interaction. Upon X-ray irradiation, more photoelectrons and Auger electrons are generated in the vicinity of the nanoparticles, which cause water ionization and lead to the formation of free radicals that damage the DNA of adjacent cancer cells. By attaching a large amount of gold nanoparticles on cancer cells, the total X-ray dose required for DNA damage and cell killing can be reduced. Due to their controllable structure and composition, multilayer microdisks can be a viable choice for enhanced radiation therapy with nanoparticles.

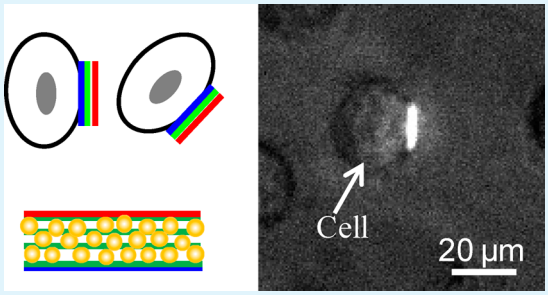

KEYWORDS: *multilayer microdisks, gold nanoparticles, cancer cells, X-ray radiation therapy, dose enhancement*

INTRODUCTION

Radiation therapy with an ionizing X-ray is an important component of cancer treatments. It can be used for primary therapy of localized tumors and for adjuvant and palliative therapy to relieve symptoms from later stage or metastatic diseases.[1−3] Although recent advances that incorporate physics, biology, and clinical aspects of radiation therapy have considerably improved the accuracy and efficiency of the dose delivery to the targeted tissue,[4−7] a major challenge of radiation therapy, i.e., to deliver radiation accurately to malignant tissues while minimizing damage to normal tissues, remains.[4] Once absorbed, X-ray photons in radiation therapy produce photoelectrons and Auger electrons, which can cause ionization of water molecules to generate reactive free radicals.[8,9] The free radicals can diffuse through chain reactions inside cells and cause damage of DNA in mitochondria and nuclei by extracting hydrogen atoms from ribose sugars, leading to cleavage of the DNA backbone.[10−13] Due to their similar amount of water content, tumors and normal tissue have similar yields of free radicals upon irradiation.

A variety of X-ray radiation techniques have been used to minimize dose on normal cells or maximize dose on cancer cells.[4,5,14] The dose can be fractionated over time to allow normal cells to recover, while cancer cells that are relatively radioresistive in the first treatment move into a relatively radiosensitive phase of cell cycle in the next treatment; the dose can be fractionated over space to intersect at tumors from several directions to spare normal cells along the beam path.[15] Image-guided radiation therapy and intensity-modulated radiation therapy can be used to maximize X-ray doses on tumors and conform the tumor's 3D shape with multiple beamlets of different intensity, respectively.[16,17] Alternative methods can be used to improve discrimination between tumor and normal tissues.[18,19] Radioprotective drugs have been used as free radical scavengers to protect normal cells from damage.[1,20] Radiosensitizers such as oxygen, oxygen carrying blood substitutes, and radiosensitive drugs have been used to enhance the effects of given X-ray doses.[21] In particular, due to their large mass energy absorption coefficients, nanoparticles of heavy elements such as gold and platinum have been studied with the intention to enhance X-ray contrasts between normal and cancer cells.[14,22,23,24] Although single gold nanoparticles can be delivered to cells for radiation therapy, free radicals generated around cells in some cases may not be sufficient to damage DNA and the uptake of nanoparticles by cells usually is influenced by the surface chemistry of nanoparticles or cell type.[25,26] On the other hand, if hundreds of thousands of nanoparticles could be placed in the vicinity of the cells, a large amount of free radicals will be available for DNA damage, and the total X-ray dose can be reduced to receive the same effect.[27]

This paper describes a method to deliver a large amount of radiosensitizing nanoparticles to tumor cells by packing nanoparticles into polyelectrolyte microdisks that will attach on the surfaces of cancer cells (Figure 1).[28] The microdisks are made by integrating microcontact printing and layer-by-layer assembly, and each microdisk contains over 10^5 gold nanoparticles. These microdisks can be released by dissolving PVA film in water and attached onto the cell surface by electrostatic

Received: October 8, 2014
Accepted: February 13, 2015
Published: February 13, 2015

DOI: 10.1021/am506866a
ACS Appl. Mater. Interfaces 2015, 7, 4518−4524

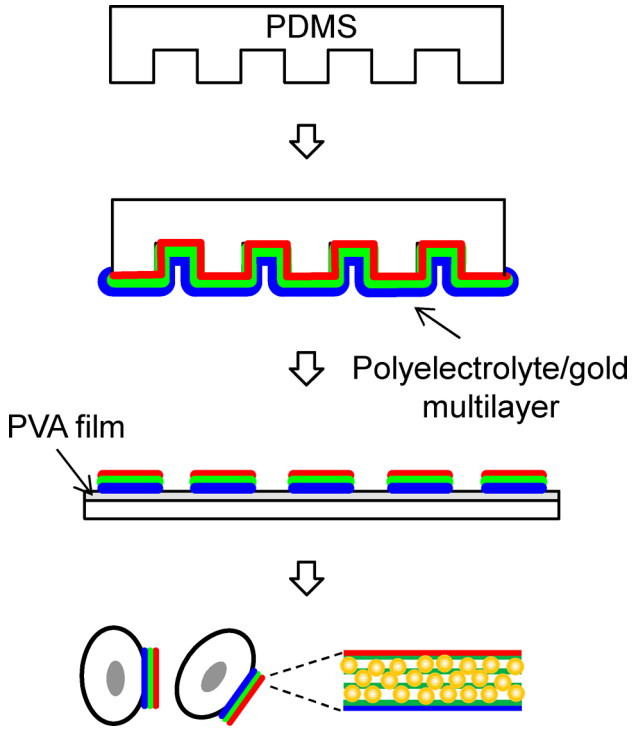

Figure 1. Gold nanoparticle-loaded microdisks for enhanced radiation therapy.

interactions. Upon X-ray irradiation, a higher level of DNA damage can be induced in cells. The enhanced DNA damage in the presence of X-ray radiation and nanoparticle-loaded microdisks has been confirmed with the single cell array based halo assay, accumulation of DNA repair proteins at break sites, and the micronucleus assay.

EXPERIMENTAL SECTION

Poly(allylamine hydrochloride) (PAH, 15 000 Da), polysodium 4-styrenesulfonate (PSS) (70 000 Da), polydiallyl-dimethylammonium chloride (PDAC) (100 000–200 000 Da), and poly(vinyl alcohol) (PVA, 20 000–70 000 Da) were purchased from Aldrich. Polydimethylsiloxane (PDMS Sylgard 184) was from Dow-Corning. PDMS stamps were prepared by casting PDMS prepolymer and curing agent on solid masters made by photolithography. Rhodamine isothiocyanate (RITC), fluorescein isothiocyanate (FITC), propidium iodide (PI), 4′,6-diamidino-2-phenylindole (DAPI), and gold nanoparticles (13 nm diameter) were obtained from Sigma. SYBR green fluorescence dye was from Invitrogen. Antiphospho-Histone γ-H_2AX antibody and antirabbit IgG-FITC antibody were obtained from Sigma. Cytokinesis B was from VWR.

PAH was labeled with FITC or RITC by reacting with FITC or RITC in water at molar ratio of 3000:1 (PAH repeat units and FITC or RITC molecules) for 24 h at room temperature. Three human cancer cell lines, A172 (human glioblastoma cells), TIB-152 (Jurkat cells), and K562 (human erythromyeloblastoid leukemia cells) were obtained from American Type Culture Collection (ATCC Manassas, VA) and cultured in standard conditions (5% CO_2 at 37 °C) in RPMI-1640 medium supplemented with 10% (v/v) fetal bovine serum and 1% (v/v) penicillin/streptomycin. Cell growth was quantified by counting cell number within a certain time.

Aqueous polyelectrolyte solutions used to make microdisks contained 1 wt % PAH-FITC (pH 5.8), 1 wt % PAH (pH 4.3), 1 wt % PSS (pH 5.8), and 1% wt PDAC (pH 4.6), as well as 150 mM NaCl. To fabricate gold nanoparticle-loaded microdisks, a PDMS stamp bearing an array of micropillars was soaked inside a polyelectrolyte solution for 12 min in order to deposit polyelectrolytes, followed by washing for 1 min with water. In order to deposit nanoparticles, a 0.5 mL aqueous suspension of nanoparticles was added on the stamp and kept for 45 min, followed by washing for 1 min with water. These steps were repeated until a desired number of layers was formed on the stamp. The stamp was then exposed to water vapor generated from a 37 °C water bath for 5 s and then brought into contact with a glass substrate coated with PVA film. After being kept in contact for 45 s, the stamp was peeled off from the substrate and exposed to water vapor generated by a 37 °C water bath for 25 s to release microdisks. Cells in medium were mixed with the microdisks and shaken gently for 3 min to allow attachment of the microdisks onto the cells.

Cells attached on the microdisks were exposed to X-ray irradiation (40 kV, 100 μA, and 80 mGy/min). The X-ray radiation is generated from a mini-X-ray generator (Amptek, Bedford, MA) operated at 40 kV and 100 μA with silver target. Dosage of the X-ray is calibrated with a radiation meter, where the X-ray can be evenly distributed over an

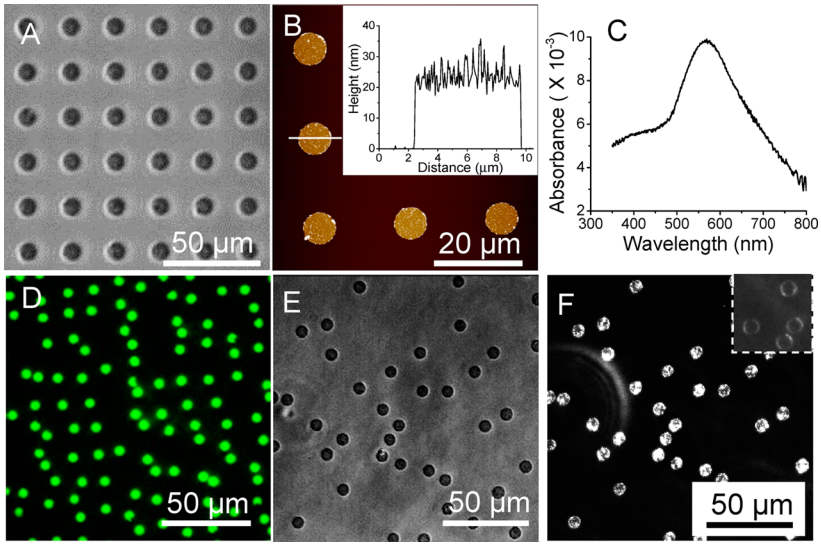

Figure 2. Phase contrast image of microdisk array on PVA coated glass (A); AFM image of microdisks on mica (B) and cross section of one microdisk (inset); UV–vis spectrum of nanoparticle-loaded microdisks attached on glass substrate (C); fluorescence (D), phase contrast (E), and dark field (F) images of released microdisks; dark field image of microdisks that do not contain gold nanoparticles (F inset).

DOI: 10.1021/am506866a
ACS Appl. Mater. Interfaces 2015, 7, 4518–4524

area of 6 × 6 cm^2. The X-ray dose and irradiation time have a linear relation when the tube is located at a vertical distance of 5 cm. Five min of X-ray irradiation will provide a 1.25Gy radiation dose on the whole irradiation area. DNA damage in cells has been quantified with the HaloChip assay,[29] micronucleus assay,[30] and expression of DNA repair protein.[31] In order to do the HaloChip assay, X-ray irradiated cells were embedded in agarose gel (0.1% mass ratio); after gel solidification, the slide was incubated with 0.3 M NaOH for 15 min at room temperature and stained with 10 μg/mL ethidium bromide (EB) for 10 min. The slide was incubated in deionized water for 3 min to remove excess EB before fluorescence observation. DNA double strand break was assessed with expression of DNA repair protein (γ-H_2XA) within the cells. Briefly, A172 cells were attached to an array of microdisks loaded with or without gold nanoparticles, where microdisks were attached on glass substrate. The cells were exposed to X-ray for 10 min and then collected from the microdisks by flushing the substrate gently and repeatedly until all cells were detached from substrate. Then, the cells were fixed with 4% paraformaldehyde in PBS for 10 min and treated with 0.1% Triton X-100 in PBS for 5 min. After incubating in blocking buffer (3% bovine serum albumin in PBS) for 1 h, primary antibody against γ-H_2XA was added and incubated at room temperature for 2 h. After rinsing with PBS, cells were incubated with FITC-conjugated secondary antibody (antirabbit IgG-FITC antibody produced in goat) for 1 h, washed with PBS, and stained with 0.2 μg/mL DAPI for 15 min, which is followed by PBS washing and fluorescence observation. Assessment of micronucleus expression was performed as follows: A172 cells attached on microdisks (without or with nanoparticles) were exposed to X-ray for 10 min. Cytokinesis B (5 μg/mL) was then added to the cell culture medium. The cells were collected by gently flushing them from the microdisks (and glass substrate) and cultured at 37 °C and 5% CO_2 for 24 h before trypsinization. Cells were then fixed with paraformaldehyde in PBS for 15 min and treated with 0.1% Triton X-100 in PBS for lysis. The nucleus in the cells were stained with DAPI (0.2 μg/mL, 15 min) and imaged under a fluorescence microscope. Fluorescence imaging of cells was performed with an Olympus IX81 microscope, with individual channels collected for DAPI, RITC, and FITC signals. Fluorescence images were merged with the software coupled with the microscope.

RESULTS AND DISCUSSION

Figure 2A is a phase contrast image of the microdisk array (5 layers of PDAC, 2 layers of nanoparticles, and 3 layers of PSS) on a PVA coated glass slide. The microdisk array has the same pattern and lateral dimensions as features on the stamp. Atomic force microscopy (AFM) imaging of microdisks reveals circular morphology and uniform dimension (Figure 2B). For microdisks with 2 layers of nanoparticles, the total thickness of multilayers and nanoparticles is ~22 nm as shown in cross section analysis of the microdisk (Figure 2B inset). The microdisk array on glass substrate is further characterized with UV–vis spectroscopy, where an absorption peak at 569 nm corresponds to plasmonic extinction of gold nanoparticles (Figure 2C). Compared to the extinction peak of gold nanoparticles in water (520 nm), the multilayer microdisks attached to glass substrates have a red shift, which is due to a change in the dielectric environment of nanoparticles after embedding in polyelectrolyte film. This result confirms that gold nanoparticles are not removed during the process, and microdisks contain gold nanoparticles. After releasing microdisks from glass substrate with water vapor, a series of optical microscopy tools are used to characterize microdisks. Figure 2D is the fluorescence image of microdisks, where the green fluorescence confirms that microdisks still contain FITC, and there is no leakage of components from microdisks. Figure 2E is a phase contrast image of microdisks, where the formation of round shaped microdisks suggests that released microdisks maintain their shapes. Figure 2F is the dark-field image of microdisks, where microdisks are bright due to Rayleigh scattering from gold nanoparticles. In contrast, microdisks that do not contain nanoparticles are not bright (Figure 2F inset). The amount of nanoparticles in each microdisk is estimated on the basis of the Lambert–Beer law: $A = \varepsilon \times \sigma$, where A is extinction, ε is extinction coefficient, and σ is molar density of nanoparticles.[28] For microdisks with diameter of 8 μm and center-to-center distance of 20 μm arranged in a square lattice, the percentage of area covered by microdisks is calculated to be 12.56% with an extinction of 0.0098. For an array of surface attached microdisks containing two layers of nanoparticles, the extinction coefficient (ε) of 10 nm diameter gold nanoparticles is 10^8 $M^{-1}cm^{-1}$.[32] The molar density of gold nanoparticles in the microdisk is 7.81 × 10^{-13} mol·cm^{-2}; thus, each microdisk (with 2 layers of nanoparticles) contains 2.36 × 10^5 nanoparticles.

Nanoparticle-loaded microdisks have been used to enhance radiation-therapy after attaching microdisks onto cell surfaces via electrostatic interactions between cell surfaces and positively charged microdisk surfaces. Figure 3A shows a dark field image

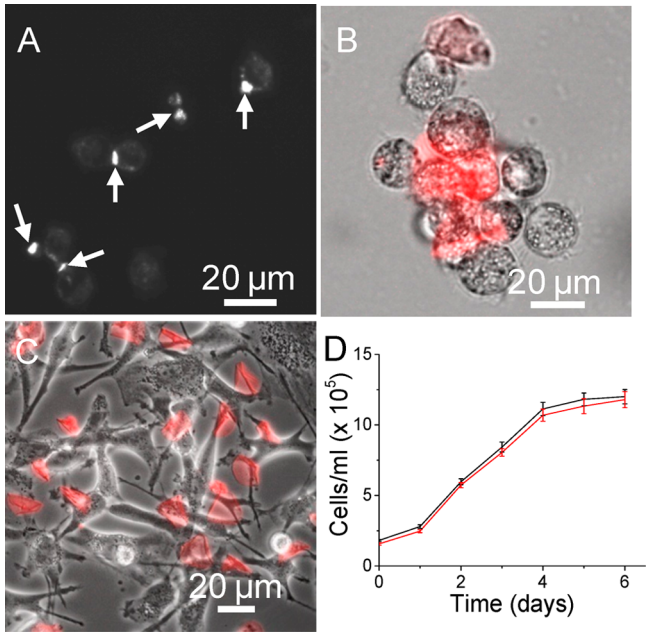

Figure 3. Dark field image of microdisks attached to suspended cancer cells (K562) in culture medium (A); fluorescence image of microdisks (red) attached with several adherent cells (A172) to form cellular aggregates (B); merged fluorescence and phase contrast image of microdisk–cell aggregates after culturing for 24 h (C); growth curves of normal cells (black curve) and microdisk attached cells (red curve) (D).

of microdisks, which are attached on the surfaces of suspended, spherically shaped cells, respectively. The arrows show microdisks attached on cell surfaces, where there is no internalization of microdisks into the cells. The diameters of the microdisks are smaller than their original ones, because microdisks are folded after attaching on cell surfaces. Some cells have two attached microdisks, while others are brought together to one microdisk. The attachment of microdisks to cells is performed in cell culture medium, which contains serum and other proteins like fetal bovine serum. The successful attachment indicates that the microdisks are not neutralized by

DOI: 10.1021/am506866a
ACS Appl. Mater. Interfaces 2015, 7, 4518–4524

these proteins. Not only suspended cells, but also the microdisks can attach onto adherent cancer cells (such as A172). In this case, both sides of the microdisks are controlled to have positive charges. The microdisks are able to attach several cells by forming cellular aggregates (Figure 3B), where cells still remain alive and can attach to the surface when cultured in medium (Figure 3C). Compared to cells without microdisks attachment, morphology and proliferation of cells with attached microdisks are not changed. The microdisks in Figure 3C are not spherical in shape because they are folded.[33] Figure 3D shows the growth dynamics of microdisks attached cells and normal cells (A172), where both cells show similar growth curves, and different phases of cell growth can be easily differentiated, indicating microdisks attachment does not affect normal functions of cells.

The viability of cancer cells (A 172) attached on an array of microdisks (without any fluorescence) has been tested with live/dead assay 2 h after attachment (Figure 4A), where

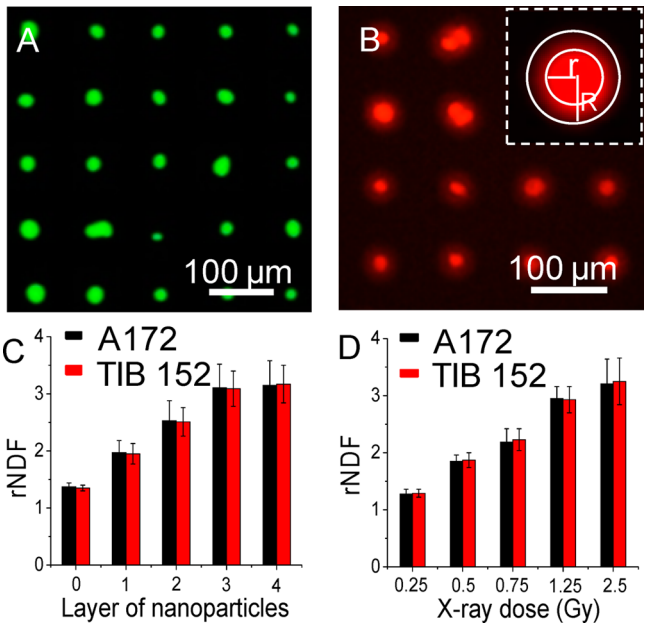

Figure 4. Live/dead assay of cells attached on microdisks array (A); fluorescence image of cancer cells (A172) after the HaloChip assay (B); rNDFs of two types of cancer cells (A172 and TIB 152) attached to microdisks with different layers of nanoparticles (C) and different X-ray doses (D).

fluorescence signals are from cells after live/dead assay. The sizes of cells sizes vary depending on cycle stage. The cells are in green color, indicating they are still alive. Our previous experiment shows that cells attached on a multilayer pattern can stay alive for at least 48 h.[34] To prove the idea of using gold nanoparticle-loaded microdisks for radiation therapy, the HaloChip assay is used to assess DNA damage induced by microdisks and X-ray at the single cell level as follows. Nanoparticle-loaded microdisks are printed on glass substrate to form an ordered array. Cells are then attached to microdisks through electrostatic interactions and are then embedded in an agarose gel. Agarose gel is used for cell culture without inducing cell damage.[35] After gel solidification, the sample is immersed in an aqueous solution of NaOH for lysis. Damaged DNA fragments self-diffuse into the gel matrix and are stained with ethidium bromide (EB), forming a diffusive ring around each nucleus. Figure 4B shows the fluorescence image of cells with haloes, where DNA in cells are damaged with X-ray and diffuse to form a halo. DNA damage is quantified with relative nuclear diffusion factor (rNDF), which is derived from areas of halo and nucleus as follows:

$$\mathrm{rNDF} = (R^2 - r^2)/r^2$$

where R and r are the radii of halo and nucleus, respectively (Figure 4B inset). Figure 4C shows rNDFs of two types of cells attached onto microdisks with different layers of nanoparticles (0, 1, 2, 3, and 4 layers) with X-ray dose of 0.75 Gy. The rNDFs increase from 1.37 ± 0.05 to 3.11 ± 0.31 (A172 cells) or from 1.35 ± 0.05 to 3.09 ± 0.41 (TIB 152 cells) when layers increase from 0 to 3. Cells attached on microdisks without nanoparticles have smaller rNDFs (1.37 ± 0.05 for A172 cells and 1.35 ± 0.05 for TIB 152 cells) than those attached to microdisks with nanoparticles (1.97 ± 0.18 to 3.11 ± 0.31 for A172 cells, and 1.95 ± 0.21 to 3.09 ± 0.41for TIB 152 cells), indicating nanoparticle enhanced radiation damage of DNA. Our previous study showed that cells (without up-taking any radiosensitive nanoparticles) irradiated with X-ray have a rNDF of 1.47 ± 0.08;[36] this is similar to cells attached onto microdisks (no gold nanoparticle loading). The dose enhancement factor (DEF) for cells attached on microdisks with 1 layer of nanoparticles with X-ray is estimated to be 1.4, as compared to cells attached onto microdisks without nanoparticles without X-ray. The estimation is based on rNDFs, where rNDF (cells attached onto microdisks with 1 layer of nanoparticles)/rNDF (cells attached onto microdisks without nanoparticles) is equal to 1.4 for both types of cells. Cells attached onto microdisks with 3 and 4 layers of nanoparticles show similar rNDFs, probably because free radicals produced by the first layer of nanoparticles cannot reach DNA in cells. Compared to DEF obtained from a survival curve,[14] the DEF calculated from rNDF is lower in value. However, this value is capable of showing the degree of DNA double strand damage.

In addition, the rNDFs of A172 and TIB 152 cells attached on microdisks (0−4 layers of nanoparticles) are close to each other, suggesting microdisks can enhance radiation damage in both adherent and suspended cells. Figure 4D shows the relation between X-ray dose and rNDF values in two cell lines. rNDFs for A172 cells and TIB 152 cells increase from 1.28 ± 0.08 to 3.21 ± 0.43 and 1.29 ± 0.07 to 3.25 ± 0.43, respectively, indicating more DNA damage can be found when X-ray dose increases. The effect of nanoparticle-loaded microdisks on X-ray radiation damage to DNA has also been assessed with a DNA double strand damage biomarker, the phosphorylated histone gamma-H2AX, which is a protein that focuses on DNA double strand damage sites and is involved in DNA damage repair. Briefly, A172 cells are attached onto microdisks without or with nanoparticles. The cells are exposed to X-ray for 10 min and collected by washing off microdisks. Primary and fluorescent labeled secondary antibodies are added sequentially in cell culture medium. The secondary antibodies are conjugated with fluorescein, which allows quantification of γ-H2AX expression by measuring fluorescence intensity. Cells irradiated on microdisks without nanoparticles with X-rays show weak green fluorescence (blue color is due to DAPI staining of DNA), indicating a small amount of γ-H2AX (Figure 5A). Cells irradiated on microdisks with nanoparticles with X-rays show strong γ-H2AX expression (Figure 5B), where the fluorescence signal from DAPI stained DNA is artificially reduced to highlight the green color. The green

DOI: 10.1021/am506866a
ACS Appl. Mater. Interfaces 2015, 7, 4518−4524

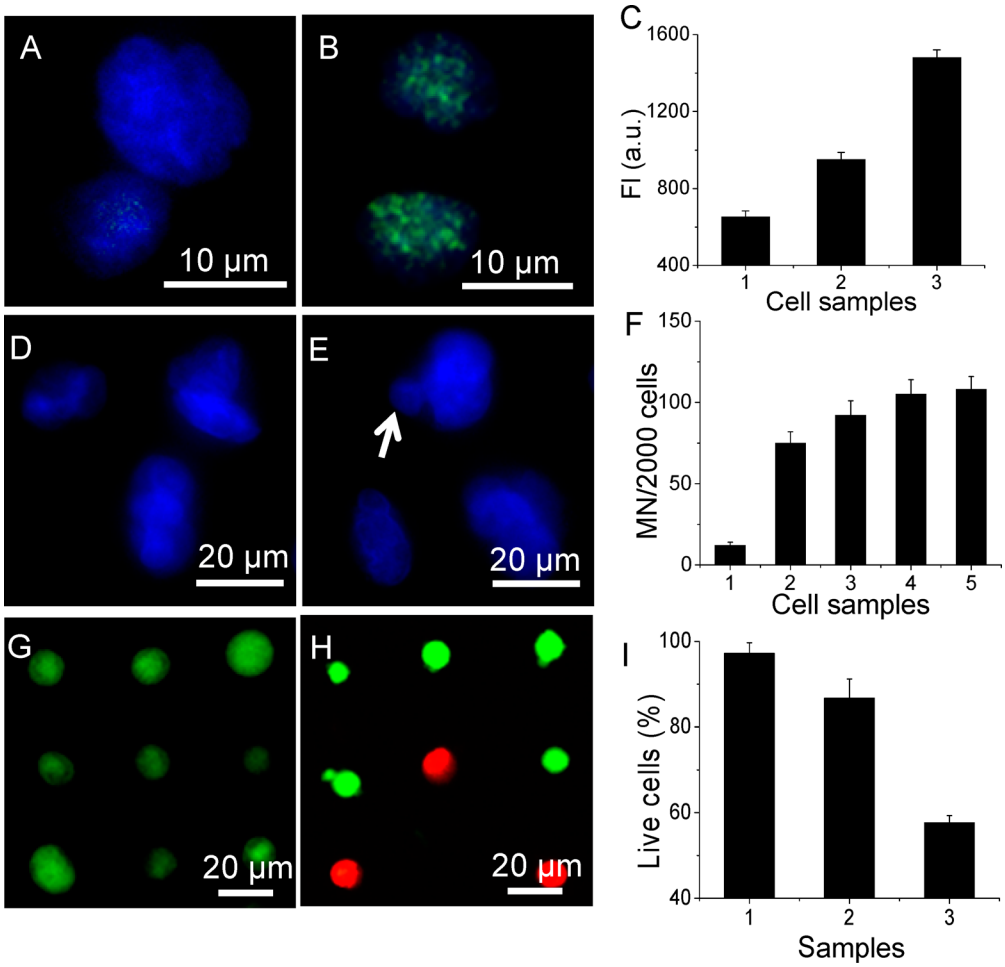

Figure 5. Fluorescence images of cells attached on microdisks that do not contain nanoparticles (A) and cells attached on microdisks that contain nanoparticles (B), after X-ray radiation and staining with DAPI and FITC-labeled γ-H2AX antibody; fluorescence intensity of FITC-labeled γ-H2AX antibody expressed on cells, where 1 has no X-ray and no nanoparticles, 2 has X-ray but no nanoparticles, and 3 has X-ray and nanoparticles (C); fluorescence images of cells attached on microdisks that do not contain nanoparticles (D) and cells attached on microdisks that contain nanoparticles (E), after X-ray radiation and staining with DAPI for micronucleus analysis; micronucleus results of cells attached on microdisks that contain different layers of gold nanoparticles after X-ray irradiation (F); live/dead assay results of cells attached on microdisks without nanoparticles and with X-ray (G) and cells attached on microdisks with nanoparticles and with X-ray (H); cell viabilities in three samples (I).

fluorescence intensities of cells have been quantified with a 96 well plate reader. Figure 5C shows the fluorescence intensities of (1) cells attached on microdisks with nanoparticles and without X-ray, (2) cells attached on microdisks with X-ray and without nanoparticles, and (3) cells attached on microdisks with X-ray and with nanoparticles. Sample (1) has lower fluorescence intensity (fluorescence intensity = 653.1 ± 31.3, arbitrary unit) than the other two; sample 3 has higher fluorescence intensity (fluorescence intensity = 1479.2 ± 71.2, arbitrary unit) than sample (2) (fluorescence intensity = 951.5 ± 37, arbitrary unit). Because γ-H2AX is related to DNA double strand breaks, these results confirm that nanoparticles in microdisks can enhance radiation induced double strand break of DNA.

The effect of nanoparticle-loaded microdisks on X-ray radiation damage to the nucleus has been assessed with the micronucleus assay.[30] Briefly, cells are attached on the microdisks array with or without nanoparticles on glass substrate, irradiated with X-ray and incubated at 37 °C in 5% CO_2 for 24 h, and then fixed with 4% para-formaldehyde in PBS for 10 min and treated with 0.1% Triton X-100 in PBS for 5 min. Cell nuclei are stained with DAPI. Cells irradiated on microdisks (nanoparticle-loaded) with X-rays have shown less micronuclei than those irradiated on microdisks with nanoparticles (Figure 5D,E). The arrows in Figure 5E indicate micronucleus from each cell after irradiation. The number of nuclei per 2000 cells are counted as shown in Figure 5F, where samples #1–#5 represent cells attached to microdisks with zero, one, two, three, and four layers of nanoparticles. Cells radiated on microdisks without nanoparticles (#1) have only 12 micronuclei per 2000 cells, which is lower than those irradiated on microdisks with nanoparticles. The number of micronuclei per 2000 cells increases with the layer of nanoparticles in microdisks. No significant difference exists between cells radiated on microdisks with three and four layers of nanoparticles. This is probably because nanoparticles in the first layer in microdisks are far away from nucleus, and free radicals produced by X-ray on these nanoparticles cannot reach the nuclei of cells.

The effect of nanoparticle-loaded microdisks on X-ray radiation killing of cells has been assessed. TIB 152 cells have been attached to microdisks loaded with or without nanoparticles through electrostatic interaction. After exposure to X-ray for 15 min, cells are incubated at 5% CO_2 at 37 °C for 24 h

DOI: 10.1021/am506866a
ACS Appl. Mater. Interfaces 2015, 7, 4518–4524

and then assessed with the live/dead assay. Figure 5G shows cells attached on microdisks that do not have nanoparticles, where the green color indicates that cells are alive. Figure 5H shows cells attached on microdisks that have nanoparticles, where cells in the red color are dead; some microdisks do not have cells attached, because dead cells detach from microdisks. Figure 5I shows cell viabilities in three samples: cells attached on microdisks with nanoparticles and without X-ray (1), cells attached on microdisks without nanoparticles and with X-ray (2), cells attached on microdisks with nanoparticles and with X-ray (3). Cells in sample (1) have a viability ratio of 97.2 ± 2.5% for over 36 h, while cells in sample 3 have a lower viability ratio (57.6 ± 1.7%) than those in sample (2) (86.7 ± 4.5%), indicating more cells are killed due to the combined effect of X-ray and nanoparticles. Rahman et al.[14] delivered colloidal gold nanoparticles to cells for enhanced radiation therapy, where up to 53% of cells are viable when 1.25 Gy of X-ray is used, depending the amount of gold nanoparticles added. This value is similar to our data (57.6 ± 1.7%). Compared to nanoparticles in single form, the microdisks are capable of delivering a huge and quantifiable amount of nanoparticles to cancer cells, therefore allowing one to generate free radicals in a controllable manner. On the other hand, it needs to be emphasized that the technique (layer-by-layer assembly) used in this work allows a combination of multiple types of nanoparticles, or nanoparticle−drug combinations to be colocally delivered to the tumor site, which also allows multiple mode therapeutics of cancer.

CONCLUSION

This paper has proved the concept of using microdisks that contain gold nanoparticles to enhance X-ray radiation killing of cancer cells. HaloChip has confirmed that nanoparticle-loaded microdisks can cause more DNA damage upon X-ray radiation. The increased fluorescence signal of DNA repair protein (γ-H2AX) indicates more double strand breaks in DNA of X-ray irradiated cells. The micronucleus assay indicates the genome level damage of cells. Cells irradiated on microdisks (nanoparticle-loaded) with X-rays have shown less micronuclei than those irradiated on microdisks with nanoparticles. More cells can be killed due to the combined effect of X-ray radiation and nanoparticles.

AUTHOR INFORMATION

Corresponding Authors

*E-mail: liy.ma@neu.edu.

*E-mail: m.su@neu.edu.

Notes

The authors declare no competing financial interest.

ACKNOWLEDGMENTS

This project is supported by a NSF CAREER award (1055599) and a NIH Director's New Innovator Award (1DP2EB016572).

REFERENCES

(1) Milas, L.; Murray, D.; Brock, W. A.; Meyn, R. E. Radioprotectors in Tumor Radiotherapy: Factors and Settings Determining Therapeutic Ratio. *Pharmacol. Ther.* **1988**, *39*, 179−187.

(2) Elshaikh, M.; Ljungman, M.; Haken, R. T.; Lichter, A. S. Advances in Radiation Oncology. *Annu. Rev. Med.* **2006**, *57*, 19−31.

(3) Hainfeld, J. F.; Dilmanian, F. A.; Slatkin, D. N.; Smilowitz, H. M. Radiotherapy Enhancement with Gold Nanoparticles. *J. Pharm. Pharmacol.* **2008**, *60*, 977−985.

(4) Lawrence, T. S. Radiation Sensitizers and Targeted Therapies. *Oncology* **2003**, *17*, 23−28.

(5) Jain, M.; Venkatraman, G.; Batra, S. Cell-Penetrating Peptides and Antibodies: A New Direction for Optimizing Radioimmunotherapy. *Eur. J. Nucl. Med. Mol. I* **2007**, *34*, 973−977.

(6) Liu, C.-J.; Wang, C.-H.; Chien, C.-C.; Yang, T.-Y.; Chen, S.-T.; Leng, W.-H.; Lee, C.-F.; Lee, K.-H.; Hwu, Y.; Lee, Y.-C.; Cheng, C.-L.; Yang, C.-S.; Chen, Y. J.; Je, J. H.; Margaritondo, G. Enhanced X-ray Irradiation-Induced Cancer Cell Damage by Gold Nanoparticles Treated by a New Synthesis Method of Polyethylene Glycol Modification. *Nanotechnology* **2008**, *19*, 295104−295109.

(7) Jain, S.; Coulter, J. A.; Hounsell, A. R.; Butterworth, K. T.; McMahon, S. J.; Hyland, W. B.; Muir, M. F.; Dickson, G. R.; Prise, K. M.; Currell, F. J.; O'Sullivan, J. M.; Hirst, D. G. Cell-Specific Radiosensitization by Gold Nanoparticles at Megavoltage Radiation Energies. *Int. J. Radiat. Oncol. Biol. Phys.* **2011**, *79*, 531−539.

(8) Schwarz, P. F.; Turro, N. J.; Bossmann, S. H.; Braun, A. M.; Wahab, A. M. A. A.; Durr, H. A New Method to Determine the Generation of Hydroxyl Radicals in Illuminated TiO_2 Suspensions. *J. Phys. Chem. B* **1997**, *101*, 7127−7134.

(9) Farokhzad, O. C.; Jon, S.; Khademhosseini, A.; Tran, T.-N. T.; LaVan, D. A.; Langer, R. Nanoparticle-Aptamer Bioconjugates: A New Approach for Targeting Prostate Cancer Cells. *Cancer Res.* **2004**, *64*, 7668−7672.

(10) Comporti, M. Three Models of Free Radical-Induced Cell Injury. *Chem. Biol. Interact.* **1989**, *72*, 1−56.

(11) Balasubramanian, B.; Pogozelski, W. K.; Tullius, T. D. DNA Strand Breaking by the Hydroxyl Radical Is Governed by the Accessible Surface Areas of the Hydrogen Atoms of the DNA Backbone. *Proc. Natl. Acad. Sci. U. S. A.* **1998**, *95*, 9738−9743.

(12) Cho, S. Estimation of Tumour Tose Enhacement Due to Gold Nanoparticles duringTypical Radiation Treatments: a Preliminary Monte Carlo Study. *Phys. Med. Biol.* **2005**, *50*, N163−N173.

(13) Fujii, K.; Shikazono, N.; Yokoya, A. Nucleobase Lesions and Strand Breaks in Dry DNA Thin Film Selectively Induced by Monochromatic Soft X-rays. *J. Phys. Chem. B* **2009**, *113*, 16007−16015.

(14) Rahman, W. N.; Bishara, N.; Ackerly, T.; He, C. F.; Jackson, P.; Wong, C.; Davidson, R.; Geso, M. Enhancement of Radiation Effects by Gold Nanoparticles for Superficial Radiation Therapy. *Nanomed.: Nanotechnol., Biol. Med.* **2009**, *5*, 136−142.

(15) Teh, B. S.; Woo, S. Y.; Butler, E. B. Intensity Modulated Radiation Therapy (IMRT): A New Promising Technology in Radiation Oncology. *Oncologist* **1999**, *4*, 433−442.

(16) Jaffray, D.; Kupelian, P.; Djemil, T.; Macklis, R. M. Review of Image-Guided Radiation Therapy. *Expert Rev. Anticancer Ther.* **2007**, *7*, 89−103.

(17) Warlick, W. B. Image-Guided Radiation Therapy: Techniques and Strategies. *J. Community Supportive Oncol.* **2008**, *5*, 86−92.

(18) Chau, Y.; Tan, F. E.; Langer, R. Synthesis and Characterization of Dextran-Peptide-Methotrexate Conjugates for Tumor Targeting via Mediation by Matrix Metalloproteinase II and Matrix Metalloproteinase IX. *Bioconjugate Chem.* **2004**, *15*, 931−941.

(19) Ghosh, A.; Heston, W. D. W. Tumor Target Prostate Specific Membrane Antigen (PSMA) and Its Regulation in Prostate Cancer. *J. Cell. Biochem.* **2004**, *91*, 528−539.

(20) Hosseinimehr, S. J. Trends in the Development of Radioprotective Agents. *Drug Discovery Today* **2007**, *12*, 794−805.

(21) Wardman, P. Chemical Radiosensitizers for Use in Radiotherapy. *Clin. Oncol.* **2007**, *19*, 397−417.

(22) Li, J.; Schneider, W.-D.; Berndt, R.; Crampin, S. Electron Confinement to Nanoscale Ag Islands on Ag(111): A Quantitative Study. *Phys. Rev. Lett.* **1998**, *80*, 3332−3335.

(23) Hainfeld, J. F.; Slatkin, D. N.; Smilowitz, H. M. The Use of Gold Nanoparticles to Enhance Radiotherapy in Mice. *Phys. Med. Biol.* **2004**, *49*, N309−N315.

(24) McMahon, S. J.; Hyland, W. B.; Muir, M. F.; Coulter, J. A.; Jain, S.; Butterworth, K. T.; Schettino, G.; Dickson, G. R.; Hounsell, A. R.; O'Sullivan, J. M.; Prise, K. M.; Hirst, D. G.; Currell, F. J. Biological

DOI: 10.1021/am506866a
ACS Appl. Mater. Interfaces 2015, 7, 4518−4524

Consequences of Nanoscale Energy Deposition Near Irradiated Heavy Atom Nanoparticles. *Sci. Rep.* **2011**, *1*, 18−27.
(25) Albanese, A.; Chan, W. C. W. Effect of Gold Nanoparticle Aggregation on Cell Uptake and Toxicity. *ACS Nano* **2011**, *5*, 5478−5489.
(26) Dykman, L. A.; Khlebtsov, N. G. Uptake of Engineered Gold Nanoparticles into Mammalian Cells. *Chem. Rev.* **2014**, *114*, 1258−1288.
(27) Hossain, M.; Su, M. Nanoparticle Location and Material-Dependent Dose Enhancement in X-ray Radiation Therapy. *J. Phys. Chem. C* **2012**, *116*, 23047−23052.
(28) Zhang, P. P.; Xia, J. F.; Wang, Z. B.; Guan, J. J. Gold Nanoparticle-Packed Microdisks for Multiplex Raman Labelling of Cells. *Nanoscale* **2014**, *6*, 8762−8768.
(29) Qiao, Y.; Wang, C. M.; Su, M.; Ma, L. Y. Single Cell DNA Damage/Repair Assay Using HaloChip. *Anal. Chem.* **2012**, *84*, 1112−1116.
(30) Holland, N.; Bolognesi, C.; Kirsch-Volders, M.; Bonassi, S.; Zeiger, E.; Knasmueller, S.; Fenech, M. The Micronucleus Assay in Human Buccal Cells as a Tool for Biomonitoring DNA Damage: The HUMN Project Perspective on Current Status and Knowledge Gaps. *Mutat. Res., Rev. Mutat. Res.* **2008**, *659*, 93−108.
(31) di Fagagna, F. D.; Reaper, P. M.; Clay-Farrace, L.; Fiegler, H.; Carr, P.; von Zglinicki, T.; Saretzki, G.; Carter, N. P.; Jackson, S. P. A DNA Damage Checkpoint Response in Telomere-Initiated Senescence. *Nature* **2003**, *426*, 194−198.
(32) Liu, X. O.; Atwater, M.; Wang, J. H.; Huo, Q. Extinction Coefficient of Gold Nanoparticles with Different Sizes and Different Capping Ligands. *Colloids Surf., B* **2007**, *58*, 3−7.
(33) Zhang, P. P.; Guan, J. J. Fabrication of Multilayered Microparticles by Integrating Layer-by-Layer Assembly and Micro-Contact Printing. *Small* **2011**, *7*, 2998−3004.
(34) Wang, Z. B.; Zhang, P. P.; Kirkland, B.; Liu, Y. R.; Guan, J. J. Microcontact Printing of Polyelectrolytes on PEG Using an Unmodified PDMS Stamp for Micropatterning Nanoparticles, DNA, Proteins and Cells. *Soft Matter* **2012**, *8*, 7630−7637.
(35) Xu, G.; Yin, F.; Wu, H.; Hu, X.; Zheng, L.; Zhao, J. In Vitro Ovarian Cancer Model Based on Three-Dimensional Agarose Hydrogel. *J. Tissue Eng.* **2014**, *5*, DOI: 10.1177/2041731413520438.
(36) Zhang, P. P.; Qiao, Y.; Wang, C. M.; Ma, L. Y.; Su, M. Enhanced Radiation Therapy with Internalized Polyelectrolyte Modified Nanoparticles. *Nanoscale* **2014**, *6*, 10095−10099.

DOI: 10.1021/am506866a
ACS Appl. Mater. Interfaces 2015, 7, 4518−4524